Reliability Engineering and System Safety 256 (2025) 110671

Contents lists available at ScienceDirect

Reliability Engineering and System Safety

journal homepage: www.elsevier.com/locate/ress

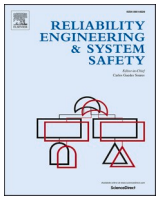

Multi-objective maintenance strategy for complex systems considering the maintenance uncertain impact by adaptive multi-strategy particle swarm optimization

Yadong Zhang [a,b], Shaoping Wang [a,d], Enrico Zio [b,e], Chao Zhang [a,c,d,*], Hongyan Dui [f], Rentong Chen [a,b]

[a] School of Automation Science and Electrical Engineering, Beihang University, Beijing 100191, PR China
[b] Energy Department, Politecnico di Milano, Via La Masa 34, Milano 20156, Italy
[c] Research Institute for Frontier Science, Beihang University, Beijing 100191, PR China
[d] Ningbo Institute of Technology, Beihang University, Ningbo 315800, PR China
[e] MINES ParisTech, PSL Research University, CRC, Sophia Antipolis, France
[f] School of Management Engineering, Zhengzhou University, Zhengzhou 450001, PR China

ARTICLE INFO

Keywords:
Maintenance
Uncertainty
Multi-objective optimization
Pareto solution optimization

ABSTRACT

Effective maintenance optimization strategies are crucial for improving the complex equipment reliability and reducing the maintenance costs. However, the effectiveness of the maintenance procedures applied to industrial equipment is affected by uncertainty, e.g. due to the professional skills of maintenance personnel, the actual condition of the equipment being maintained. The quantification of the uncertainty on the effect of maintenance has practical significance and must be accounted in the development of maintenance strategies for reducing equipment probability of failure. This paper proposes a multi-objective maintenance strategy considering the uncertain impact of the maintenance actions. The impact of maintenance actions on the reliability of components is first studied and a reliability assessment model is developed, which considers the skill of maintenance personnel and the actual condition of the equipment. To optimize the multi-objective maintenance strategy, a multi-strategy particle swarm optimization (MS-PSO) algorithm is proposed. Two case studies are considered to verify the effectiveness of the proposed approach for multi-objective maintenance strategy optimization. In the case studies considered, it turns out that the maintenance cost rate (MCR) is reduced throughout the system life cycle and the cumulative availability is improved.

1. Introduction

Equipment and engineering systems are exposed to failures due to harsh external environments [1,2] and internal degradation of the components [3], which may cause significant economic losses, and even human injuries and fatalities [4,5]. This motivates industry requirements for high system reliability and security [6,7]. Maintenance is necessary for ensuring system reliability, availability, and equipment safety. However, the development of maintenance strategies is challenging.

Existing maintenance strategies include corrective maintenance (CM) [8], scheduled preventive maintenance (PM) [9,10], opportunistic maintenance (OM) [11], condition-based maintenance (CBM) [12,13], and predictive maintenance (PdM) [14]. Many related studies have been conducted. For instance, considering that the failure type affects the system maintenance costs, Dui et al. [15] proposed a variable system cost method considering the full life cycle; they developed PM strategies by identifying component failure modes and integrating them into the full life cycle assessment. Considering the insufficient reliability utilization caused by premature maintenance, Lu et al. [16] proposed a multi-objective optimization model for OM strategy, and evaluated the economic benefits and failure risks. Levittin et al. [17] analyzed the expected task cost composition of incomplete production by a system and minimized it. Zhang et al. [18] proposed a cost-based maintenance priority model for assisting in the selection of the components for PM and reducing the system maintenance costs. The aforementioned

* Corresponding author.
E-mail address: czhangstar@gmail.com (C. Zhang).

https://doi.org/10.1016/j.ress.2024.110671
Received 8 June 2024; Received in revised form 14 November 2024; Accepted 18 November 2024
Available online 28 November 2024

researches focus on the development and optimization of maintenance strategies centered on the maintenance costs.

However, formulating an effective maintenance strategy is not only about seeking the lowest maintenance cost, especially for complex equipment and systems [19,20]. It may require the consideration of also other factors, such as the availability and reliability [21]. Zuo et al. [22] proposed a continuous bi-objective optimization model for planning the risk-related resources and developed a rule-based metaheuristic algorithm, showing the importance of risk responses in project risk management. Cai et al. [23] considered that the degradation of structural systems is caused by multiple factors and proposed a hybrid method to predict the life of submarine pipelines to provide a basis for condition-based maintenance. Wang et al. [24] considered the impact of the failure modes of leakage and burst on pipeline maintenance, and established a multi-objective maintenance optimization model for pipelines with availability and cost rate as optimization objectives. Han et al. [25] developed two dynamic risk models and proposed a systematic multi-objective optimization framework for the optimization of PM intervals to ensure the safety of critical equipment in offshore facilities. Wei et al. [26] proposed a multi-objective optimization decomposition strategy for complex equipment of aero-engines, eliminating the need for pre-established maintenance thresholds for different objectives.

For many complex equipment and systems, the development and actuation of the maintenance strategies is affected by various uncertainties, for example, due to the random process of degradation and the operational and environmental combinations. Chen et al. [27] considered that insufficient knowledge of maintenance and degradation mechanisms would lead to epistemic uncertainty of maintenance parameters, and proposed an OM optimization model for continuous manufacturing systems by introducing an opportunity time window to constrain production. Considering the increased uncertainty in the operation process of the control system as the complexity increases, Liu et al. [28] proposed a hybrid multi-stage control system rule constraint prediction method to make up for the lack of understanding of the real degradation process. Considering that the lack of available information on components or systems will lead to cognitive uncertainty and thus affect the assessment of system importance, Chen et al. [29] proposed an uncertainty comprehensive importance measure to effectively evaluate the importance of components. Li et al. [30] considered that these uncertainties such as randomly occurring shocks would cause additional damage to equipment, and proposed a reliability model based on Markov regeneration process to explain their impact on reliability modeling. Considering the uncertainty of machine failures, Ruiz-Rodríguez et al. [31] formulated a stochastic scheduling problem to maximize machine uptime by decreasing the mean time to repair. Li et al. [32] proposed a comprehensive decision-making framework to consider component failure time uncertainty, and used the Monte Carlo method [33] to generate random scenarios. Considering the uncertainty of the impact of external shocks on the degradation rate, Zhang et al. [34] proposed a component maintenance priority selection strategy to guide system maintenance. Some studies have also considered the uncertain effects of external disasters and random shocks, incorporating them into the maintenance optimization of subsea control systems [35,36].

In practice, the components of a system undergo several possible imperfect maintenances during the lifetimes, until a perfect maintenance is carried out, i.e. until the component is replaced with new ones. The reliability of components will be improved after repairs, but the technical level of different maintenance personnel will have a great impact on the quality of component repairs. These uncertainties directly affect the evaluation of system reliability and availability, which affects the formulation of maintenance strategies. Neglecting the impact of uncertain on maintenance can lead to unreasonable maintenance strategies, which can have negative consequences, including unjustified maintenance expenses and production losses. In the development of maintenance strategies, the consideration of these uncertainties and the quantitative analysis of their impact on the reliability modeling and maintenance optimization are lacking, especially in the existing multi-objective maintenance strategies. Therefore, they should be further studied.

In addition, in order to solve the optimization problem in maintenance strategies, intelligent algorithms are required to determine the optimal solution in multi-objectives. The commonly used algorithms for solving multi-objective optimization include the genetic algorithm (GA) [37] and PSO algorithm [38,39]. The GA search starts from the group, and it is able to conduct simultaneous comparisons of multiple individuals, which has broad application prospects. However, the results of the search depend on the initialization population and evaluation function. Therefore, the accurate choice of parameters significantly affects the quality of the solution, and most of the existing methods for the selection of these parameters rely on the experience. In addition, a complex problem requires high computational load and computing resources. The basic PSO algorithm evaluates the quality of the solution through fitness. Therefore, it has simpler rules than the GA, it requires fewer parameters to be adjusted, and it can be more easily implemented. In addition, each particle in PSO is guided by its historical local and global best positions. This mechanism allows the particles to quickly converge to the optimal solution. However, many problems, such as local optimal solutions and poor diversity may occur during the optimization solution process.

The research presented in this paper considers uncertain factors in maintenance behavior, and quantitatively analyzes its impact on the reliability modeling and maintenance optimization. In addition, a multi-strategy particle swarm optimization (MS-PSO) algorithm is proposed to overcome some problems faced by the traditional PSO algorithm, i.e., falling into local optimal solutions and lacking global diversity in the multi-objective solutions. Fig. 1 shows the flowchart of the proposed multi-objective maintenance strategy. The main contributions of this paper are summarized as follows:

1) A system reliability model incorporating the uncertainty of maintenance effects is developed, along with a reliability assessment method that comprehensively accounts for both the professional skills of maintenance personnel and the condition of the components. In comparison to conventional reliability models that neglect maintenance uncertainties, the proposed approach more accurately mitigates the risk of underestimating the failure probability of maintained components.
2) A novel MS-PSO algorithm is introduced to optimize the multi-objective maintenance strategy. The performance of MS-PSO is benchmarked against NSGA-II, with the results demonstrating that the proposed MS-PSO achieves superior solution uniformity and accuracy compared to both NSGA-II and basic PSO. Specifically, the solution distribution on the Pareto front (PF) is more uniform and closely aligned with the true PF. These findings indicate that the proposed algorithm outperforms NSGA-II and PSO in terms of optimization efficiency and solution quality.
3) A multi-objective maintenance decision-making model for the life cycle management of complex systems is formulated and optimized using the proposed MS-PSO algorithm. This approach enables the optimization of maintenance time and actions, ensuring system safety while simultaneously minimizing the MCR and enhancing cumulative availability.

The remainder of this paper is organized as follows. Section 2 introduces the reliability model considering the uncertain maintenance impact and the multi-objective maintenance optimization model. Section 3 details the proposed MS-PSO algorithm, including the introduction of the adaptive weight optimization strategy and multi-weight subspace particle constraint strategy adopted to overcome the shortcomings of the basic PSO algorithm. Section 4 presents two case studies for the application of the proposed models and algorithm. Finally, the

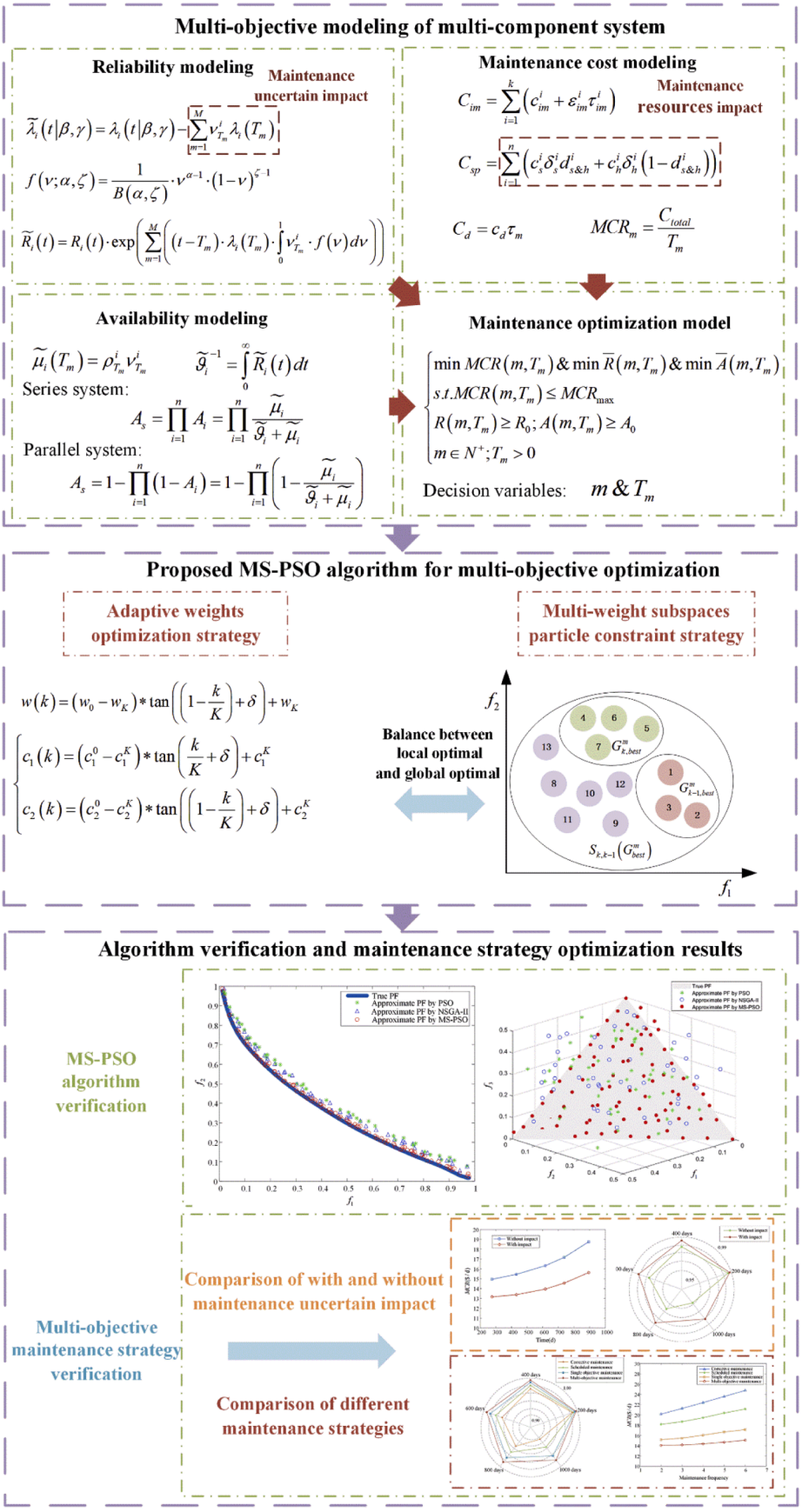

Fig. 1. Flowchart of the proposed multi-objective maintenance strategy.

conclusion and future directions of work are discussed in Section 5.

Acronyms		Symbols	
PSO	Particle swarm optimization	β_i	Shape parameter of component i
MS-PSO	Multi-strategy-particle swarm optimization	γ_i	Scale parameter of component i
MCR	Maintenance cost rate	T_m	The m-th imperfect maintenance time
CM	Corrective maintenance	$\nu^i_{T_m}$	Professional skills for m-th maintenance
PM	Preventive maintenance	$E(\nu)$	Expectation of professional skills
OM	Opportunistic maintenance	$\sigma(\nu)$	Standard deviation of professional skills
CBM	Condition based maintenance	C_{im}	Imperfect maintenance cost
PdM	Predictive maintenance	C_{pm}	Perfect maintenance cost
GA	Genetic algorithm	C_{sp}	Spare parts cost
NSGA-II	Nondominated sorting genetic algorithm-II	C_d	Downtime cost
PF	Pareto front	C_{om}	Uncertainty loss cost
PDF	Probability density function	κ_a	Penalty factor for advanced maintenance
MTTF	Mean time to failure	κ_d	Penalty factor for delayed maintenance
MTTR	Mean time to repair	τ_m	Maximum downtime for m-th maintenance
HV	Hypervolume	$\rho^i_{T_m}$	State of the component during the m-th maintenance
IGD	Inverted generational distance	$\tilde{\mu}_i(T_m)$	Repair rate of component i for the m-th time
FT	Fuel tank	m	The number of maintenance actions
EDP	Engine driven pump	w	Inertia weight
EMP	Electric motor pump	c_1	Local learning factor
FSOV	Fire shut-off valve	c_2	Global learning factor
Acc	Accumulator	$\tilde{\lambda}_i(t)$	Failure rate of component i considering maintenance actions
SV	Solenoid valve	$\tilde{R}_i(t)$	Reliability of component i considering maintenance actions
RAT	Ram air turbine	δ	Adjustment coefficient
PTU	Power transfer unit	A_s	System availability

2. Construction of multi-objective models for multi-component system

This section mainly describes the construction of multi-component system reliability model considering maintenance uncertainty and the construction of multi-objective function for a maintenance optimization model, providing a basis for the formulation and optimization of a multi-objective maintenance strategy for complex system.

2.1. Multi-component system reliability model considering the maintenance uncertain impact

The lifetime of the i th component of a mechanical system is often assumed to follow the Weibull distribution [40], whose probability density function (PDF) is:

$$f_i(t|\beta,\gamma)=\frac{\beta_i}{\gamma_i}\cdot\left(\frac{t}{\gamma_i}\right)^{\beta_i-1}\cdot\exp\left(-\left(\frac{t}{\gamma_i}\right)^{\beta_i}\right) \tag{1}$$

where β_i is the shape parameter and γ_i is the scale parameter. These parameters can be determined based on historical failure data.

The failure rate function of component i can then be expressed as

$$\lambda_i(t|\beta,\gamma)=\frac{\beta_i}{\gamma_i}\cdot\left(\frac{t}{\gamma_i}\right)^{\beta_i-1} \tag{2}$$

During the entire lifecycle operation, perfect maintenance or imperfect maintenance will generally be performed based on the state of the component. Perfect maintenance usually involves replacing parts to keep the component in perfect condition, while the imperfect maintenance involves disassembling and reassembling the parts of the component. When imperfect maintenance is performed on a component, its failure rate is reduced, which allows to extend its service life. With reference to Fig. 2, we can update the effect of imperfect maintenance on the failure rate as follows:

$$\tilde{\lambda}_i(t|\beta,\gamma)=\begin{cases}\lambda_i(t|\beta,\gamma), t<T_1\\ \lambda_i(t|\beta,\gamma)-\nu^i_{T_1}\lambda_i(T_1), T_1\le t<T_2\\ \cdots\\ \lambda_i(t|\beta,\gamma)-\sum_{m=1}^{M}\nu^i_{T_m}\lambda_i(T_m), t\ge T_M\end{cases} \tag{3}$$

where $\tilde{\lambda}_i(t|\beta,\gamma)$ is the failure rate of component i considering the maintenance actions, T_m is the time of the m-th imperfect maintenance, $\nu^i_{T_m}$ is the professional skills of the maintenance technician repairing component i for the m-th maintenance time.

Note that it is reasonable to assume that $0<\nu<1$. A large ν indicates that the maintenance technicians have good repair capacity, and a small ν indicates that the maintenance level of technician is poor. The factor ν of professional skill is a random variable, which we assume to follow beta distribution, whose PDF is [41]:

$$f(\nu;\alpha,\zeta)=\frac{1}{B(\alpha,\zeta)}\cdot\nu^{\alpha-1}\cdot(1-\nu)^{\zeta-1} \tag{4}$$

where α is the shape parameter, ζ is the scale parameter and the beta function $B(\alpha,\zeta)$ is given by:

$$B(\alpha,\zeta)=\int_0^1 t^{\alpha-1}\cdot(1-t)^{\zeta-1}dt \tag{5}$$

The expectation $E(\nu)$ and standard deviation $\sigma(\nu)$ of the beta distribution are used to represent the average operating capacity of the maintenance personnel and the uncertainty of the average skills respectively:

$$E(\nu)=\alpha/\alpha+\zeta \tag{6}$$

$$\sigma(\nu)=\sqrt{\alpha\zeta/(\alpha+\zeta)^2(\alpha+\zeta+1)} \tag{7}$$

The reliability of component i at time t can be expressed as:

$$R_i(t)=\exp\left(-\int_0^t\lambda_i(\varphi)d\varphi\right) \tag{8}$$

If component i has undergoes imperfect maintenance M times before time T_m, its reliability can be expressed as:

$$\tilde{R}_i(t)=\begin{cases}\exp\left(-\int_0^t\tilde{\lambda}_i(\varphi)d\varphi\right)=R_i(t), t<T_1\\ R_i(t)\cdot\exp\left((t-T_1)\cdot\lambda_i(T_1)\cdot\int_0^1\nu^i_{T_1}\cdot f(\nu)d\nu\right), T_1\le t<T_2\\ \cdots\\ R_i(t)\cdot\exp\left(\sum_{m=1}^{M}\left((t-T_m)\cdot\lambda_i(T_m)\cdot\int_0^1\nu^i_{T_m}\cdot f(\nu)d\nu\right)\right), t\ge T_M\end{cases} \tag{9}$$

For a series system, the reliability is then calculated as:

$$\tilde{R}_s(t)=\prod_{i=1}^{n}\tilde{R}_i(t) \tag{10}$$

and for the parallel system, the reliability is:

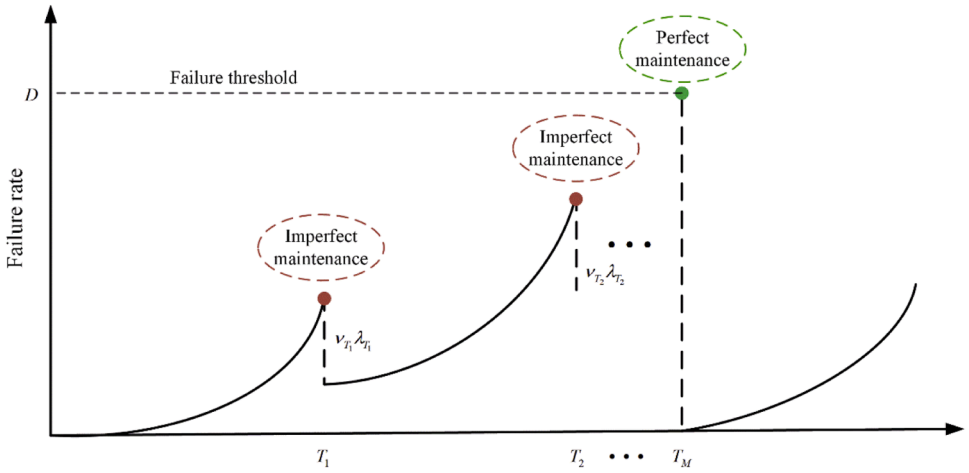

Fig. 2. Changes in component failure rate during a replacement cycle.

$$\widetilde{R}_s(t) = 1 - \prod_{i=1}^{n}(1 - \widetilde{R}_i(t)) \tag{11}$$

2.2. Maintenance cost model

The maintenance costs usually include the component replacement costs, downtime costs, spare parts ordering costs, and inspection costs, etc. These cost functions are detailed in the sequel.

(1) Imperfect maintenance cost

The imperfect maintenance costs are those costs for components that can be repaired by disassembling and reassembling the components and replacing small internal parts. It usually includes some repair costs for the maintenance personnel. The cost of the system imperfect maintenance can be expressed as:

$$C_{im} = \sum_{i=1}^{k}\left(c_{im}^{i} + \varepsilon_{im}^{i}\tau_{im}^{i}\right) \tag{12}$$

where k is the number of components of the system requiring for imperfect maintenance, c_{im}^{i} is the parts cost of the imperfect maintenance of the i th component, ε_{im}^{i} is the maintenance cost per unit time of the maintenance personnel for the imperfect maintenance of the i th component, and τ_{im}^{i} is the time needed for the imperfect maintenance of the i th component.

(2) Perfect maintenance cost

The perfect maintenance cost is the cost of replacing components with new ones, which can be expressed as:

$$C_{pm} = \sum_{i=1}^{n-k}\left(c_{pm}^{i} + \varepsilon_{pm}^{i}\tau_{pm}^{i}\right) \tag{13}$$

where n is the number of components requiring maintenance, c_{pm}^{i} is the replacement cost of the i th component, ε_{pm}^{i} is the maintenance cost per unit time of the maintenance personnel for the i th component, τ_{pm}^{i} is the downtime of replacement of the i th component.

(3) Spare parts cost

For performing the maintenance tasks, the relevant components requiring maintenance should be determined according to the maintenance plan, and the spare parts should be ordered. If spare parts are not ready when the planned maintenance time is reached, the implementation of the maintenance plan will be affected, if they become available long before the planned maintenance, storage costs are usually paid. The dispatch cost of spare parts can be expressed as:

$$C_{sp} = \sum_{i=1}^{n}\left(c_{s}^{i}\delta_{s}^{i}d_{s\&h}^{i} + c_{h}^{i}\delta_{h}^{i}\left(1 - d_{s\&h}^{i}\right)\right) \tag{14}$$

where c_{s}^{i} and c_{h}^{i} are the spare parts out-of-stock cost and holding cost for the i th component maintenance per unit time respectively, δ_{s}^{i} and δ_{h}^{i} are the corresponding out-of-stock time and holding time respectively, $d_{s\&h}^{i}$ indicating whether the spare parts for the i th maintenance component are out of stock ($d_{s\&h}^{i} = 1$) or not ($d_{s\&h}^{i} = 0$).

(4) Downtime cost

The downtime cost depends on the duration of the system down state. The maintenance times of n components requiring maintenance are $\tau_{im}^{1}, \tau_{im}^{2}, \ldots, \tau_{im}^{k}, \tau_{pm}^{1}, \tau_{pm}^{2}, \ldots, \tau_{pm}^{n-k}$. Assuming that the maintenance activities for each system component do not affect each other and they are performed in parallel, the downtime of the system depends on the longest maintenance time of a component, $\tau_m = \underset{0\le i\le n}{max}\left\{\tau_{im}^{i},\ \tau_{pm}^{i}\right\}$. Therefore, the system downtime cost can be expressed as:

$$C_d = c_d\tau_m \tag{15}$$

where c_d is the cost of production loss per unit time and τ_m is the maximum downtime for the m-th maintenance.

(5) Uncertainty loss cost

A penalty factor is introduced to represent the cost loss caused by advanced or delayed maintenance and the associated cost can be expressed as:

$$C_{om} = \kappa_a\cdot(T_m - t_a)\cdot d_a^m + \kappa_d\cdot(t_d - T_m)\cdot d_d^m \tag{16}$$

where κ_a andκ_d are the penalty factors for advanced maintenance and delayed maintenance per unit time respectively, t_a and t_d are the actual advanced maintenance time and delayed maintenance time respectively, d_a^m and d_d^m are binary variable to determine whether the m-th maintenance is advanced or delayed respectively ($d_a^m = 1\&d_d^m = 0$if advanced, $d_a^m = 0\&d_d^m = 1$ if delayed).

The total maintenance cost of the system is the sum of the aforementioned cost items:

$$C_{total} = C_{im} + C_{pm} + C_{sp} + C_d + C_{om} \tag{17}$$

The maintenance cost rate (MCR) of the system is the ratio of the total maintenance cost to the running time before the m-th maintenance:

$$MCR_m = \frac{C_{total}}{T_m} \tag{18}$$

2.3. Availability model of the system

The availability is a measure of the ability of a system or component to return to a state in which it can execute its intended function after maintenance. It is typically expressed by the ratio of the mean time to failure (MTTF) to the sum of MTTF and mean time to repair (MTTR). The repair rate of a component is usually related to its conditions, such as the number of repairs, the complexity of the component and the professionalism of the maintenance personnel, etc. Therefore, the component repair rate can be expressed as:

$$\widetilde{\mu}_i(T_m) = \rho^i_{T_m}\nu^i_{T_m}, m = 1, 2, \ldots, M \tag{19}$$

where $\rho^i_{T_m}$ is the state of the component during the m-th maintenance, which is related to its number of repairs and its complexity ($0 \le \rho^i_{T_m} \le 1$).

Therefore, the MTTR of component i can be expressed as:

$$MTTR_i = \frac{1}{\widetilde{\mu}_i} \tag{20}$$

The MTTF of a component can then be defined as:

$$MTTF_i = \int_0^\infty t f_i(t)dt \tag{21}$$

Considering the imperfect maintenance of components, their reliability is updated every time a maintenance is performed. By transformation $f(t) = d(1 - R(t))/dt$, the MTTF of component i can be rewritten as:

$$MTTF_i = \int_0^\infty \widetilde{R}_i(t)dt \tag{22}$$

where the reliability of component i at time t considering the maintenance action is derived as presented in Section 2.1.

Let $MTTF_i = \widetilde{\vartheta}_i^{-1}$, for a series system, the availability is then calculated as:

$$A_s = \prod_{i=1}^{n} A_i = \prod_{i=1}^{n} \frac{\widetilde{\mu}_i}{\widetilde{\vartheta}_i + \widetilde{\mu}_i} \tag{23}$$

and for the parallel system, the availability is [42]:

$$A_s = 1 - \prod_{i=1}^{n}(1 - A_i) = 1 - \prod_{i=1}^{n}\left(1 - \frac{\widetilde{\mu}_i}{\widetilde{\vartheta}_i + \widetilde{\mu}_i}\right) \tag{24}$$

2.4. Multi-objective maintenance optimization model

In this study, the system maintenance optimization objectives are the MCR, reliability, and availability. The decision variables are the number of maintenance actions (m) and the maintenance times (T_m). The following three scenarios for multi-objective optimization are considered:

Scenario 1: The objectives of the optimization are the minimization of the MCR and the unavailability with the constraint of reliability. The optimization model can be expressed as:

$$\begin{cases} \min MCR(m, T_m) \& \min \overline{A}(m, T_m) \\ s.t. R(m, T_m) \ge R_0 \\ m \in N^+; T_m > 0 \end{cases} \tag{25}$$

where $\overline{A}(m, T_m) = 1 - A(m, T_m)$ is the unavailability, R_0 is the constraining minimum reliability required for the system, and N^+ is the set of positive integers.

Scenario 2: The objectives of the optimization are the minimization of the MCR and the unreliability with the constraint of availability. The optimization model can be expressed as:

$$\begin{cases} \min MCR(m, T_m) \& \min \overline{R}(m, T_m) \\ s.t. A(m, T_m) \ge A_0 \\ m \in N^+; T_m > 0 \end{cases} \tag{26}$$

where $\overline{R}(m, T_m) = 1 - R(m, T_m)$ is the unreliability and A_0 is the minimum availability acceptable for the system.

Scenario 3: The objectives of the optimization are the minimization of the MCR, the unreliability and the unavailability. The optimization model can be expressed as:

$$\begin{cases} \min MCR(m, T_m) \& \min \overline{R}(m, T_m) \& \min \overline{A}(m, T_m) \\ s.t. MCR(m, T_m) \le MCR_{\max} \\ R(m, T_m) \ge R_0; A(m, T_m) \ge A_0 \\ m \in N^+; T_m > 0 \end{cases} \tag{27}$$

where $MCR_{\max}$ is the upper limit for the MCR.

3. Adaptive MS-PSO algorithm for multi-objective optimization

A multi-objective PSO algorithm is used to solve the optimization models of the three multi-objective scenarios. Compared with other algorithms, the PSO algorithm has clear advantages such as its insensitivity to initial values, high global search ability and high convergence speed. However, the PSO algorithm can fall into local optimal in the later stages. In order to solve the aforementioned problems, an adaptive MS-PSO algorithm is proposed.

3.1. Basic definition of PSO

PSO is a heuristic optimization algorithm, where each particle represents an individual solution in the search space. Particles have position and velocity in the problem domain, where individuals search for local optimal solutions, and information is exchanged between local and global. The particles having the highest performance in the group guide the individuals to search for positions, and their speed and position are adjusted through local optimality and global optimality during each iteration to determine the global optimal solution.

Assuming that N particles exist in the M-dimensional search space, and each particle represents a solution, the position and speed of the i th particle after the k-th iteration can then be expressed as:

$$\begin{cases} X_{i,k} = \left(x^1_{i,k}, x^2_{i,k}, \ldots, x^M_{i,k}\right) \\ V_{i,k} = \left(v^1_{i,k}, v^2_{i,k}, \ldots, v^M_{i,k}\right) \end{cases} \tag{28}$$

After k iterations, the local optimal position searched by the i th particle and the global optimal position searched by the group can be expressed as:

$$\begin{cases} P_{i,k,best} = \left(p_{i,k}^1, p_{i,k}^2, \ldots, p_{i,k}^M\right) \\ G_{k,best} = \left(g_k^1, g_k^2, \ldots, g_k^M\right) \end{cases} \tag{29}$$

In this study, the minimization optimization objective is denoted by $\min f(X)$. In the local optimization process, if the current fitness value of the local is greater than his historical optimal fitness value, his historical optimal position is retained. If the current fitness value of the local is less than his historical optimal fitness value, his historical optimal position is updated to the current position:

$$P_{i,k,best} = \begin{cases} X_{i,k}, f\left(X_{i,k}\right) < f\left(P_{i,k-1,best}\right) \\ P_{i,k-1,best}, f\left(X_{i,k}\right) \geq f\left(P_{i,k-1,best}\right) \end{cases} \tag{30}$$

In the basic PSO algorithm, the changes of the velocity and position of the particles at the $(k+1)$-th iteration can be expressed as:

$$\begin{cases} V_{i,k+1}^m = wV_{i,k}^m + c_1 r_1 \left(P_{i,k,best}^m - X_{i,k}^m\right) + c_2 r_2 \left(G_{k,best}^m - X_{i,k}^m\right) \\ X_{i,k+1}^m = X_{i,k}^m + V_{i,k+1}^m \end{cases} \tag{31}$$

where $m = 1,2,\ldots,M$, w is the inertia weight which represents the impact of the velocity of the previous generation of particles on the velocity of their current generation, c_1 and c_2 respectively represent the local and global learning factors indicating the weight of the next action of the particle derived from its own experience part or the experience part of other particles. r_1 and r_2 are random numbers in the range of [0 1], used to increase the randomness of the search.

3.2. Adaptive weights optimization strategy

This study adopts the PSO algorithm to solve the multi-objective optimization model. The inertia weight and learning factor of the basic PSO do not change with the number of iterations. Consequently, the algorithm is sensitive to the initial parameters value, it easily falls into local optimal, which significantly decrease the effectiveness of the global search within the solution space.

As improvement, an adaptive weight optimization strategy is here proposed, where the inertia weight and learning factor are dynamically adjusted with the number of iterations. In the early stage, a large inertia weight is used to increase the global search capacity, which allows the particles to explore new areas and escape from the local optimal. In the late stage of the search, a smaller inertia weight of the w is used to increase the local search ability, which allows the algorithm to quickly converge to the optimal solution. This adaptive weight strategy can balance the global and local search capacities, which can result in a superior optimal solution. The dynamic change of the inertia weight w with the number of iterations k can be expressed as:

$$w(k) = (w_0 - w_K) * \tan\left(\left(1 - \frac{k}{K}\right) + \delta\right) + w_K \tag{32}$$

where k and K represent the current number of iterations and the maximum number of iterations respectively, w_0 and w_K represent the initial inertia weight and the inertia weight of the maximum number of iterations respectively, δ is the adjustment coefficient and $\tan(\cdot)$ is the tan function.

The learning factor represents the weight of the next action of the particle derived from its own experience or the experience of other particles. A low value causes the particles to hover around the target area, whereas a high value makes them cross the target area. This study aims at achieving particle diversity in the initial stage and quickly converging to the global optimum in the late stage. Therefore, the weight of the local learning factors should be gradually increased, whereas that of the global learning factors should be gradually decreased, so as to more effectively balance the global and local search. The dynamic adjustment of the learning factor can be expressed as:

$$\begin{cases} c_1(k) = \left(c_1^0 - c_1^K\right) * \tan\left(\frac{k}{K} + \delta\right) + c_1^K \\ c_2(k) = \left(c_2^0 - c_2^K\right) * \tan\left(\left(1 - \frac{k}{K}\right) + \delta\right) + c_2^K \end{cases} \tag{33}$$

where c_1^0 and c_2^0 are the initial local and global learning factors respectively, c_1^K and c_2^K are the local and global learning factors of the maximum number of iterations respectively.

3.3. Multi-weight subspaces particle constraint strategy

When the PSO algorithm is in the searching process, it is usually accompanied by the loss of population diversity, which may lead to a local optimal and precocious convergence. In general, the more population diversity, the higher the probability of global convergence of the algorithm. In order to improve the diversity of the particle search process, a multi-weight subspaces particle constraint strategy is proposed to balance the local optimal and global optimal phases of search.

The strategy is based on the current global optimal particle and global optimal particle before iteration, and it also considers the particle constraint area. In this area, the weight of the particle changes with the distance (i.e., Euclidean distance). This allows to increase the diversity of the particles during the search and also increase the global performance of the PSO algorithm. The framework of the multi-weight subspaces particle constraint strategy is shown in Fig. 3.

A group of particles is initialized in space, where each particle is a potential solution. All the particles follow the current optimal particles in the solution space. Then the optimal particle is selected to update the local and global extreme values until the optimal solution of the Euclidean distance is found to establish the weight subspaces. The Euclidean distance between the two global optimal particles is computed as:

$$d_{k,k-1}\left(G_{best}^m\right) = \sum_{m=1}^{M} \left(f_m\left(G_{k,best}^m\right) - f_m\left(G_{k-1,best}^m\right)\right)^2 \tag{34}$$

where G_{best}^m is the m-dimensional global optimal particle, $f_m\left(G_{k,best}^m\right)$ is its fitness value in the k-th iteration, and $f_m\left(G_{k-1,best}^m\right)$ is its fitness value in the k-1-th iteration.

A weight subspace is constructed near the Euclidean distance of the two global optimal particles in the k-1-th and k-th iterations, and the

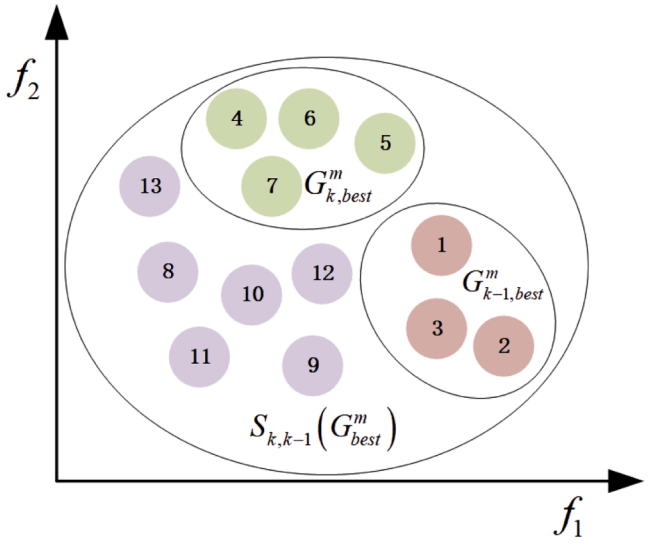

Fig. 3. Framework of the multi-weight subspaces particle constraint strategy.

particles are guided to search within this space for the most likely global optimal position. This allows to increase the efficiency of the population search. The weight subspaces of the particles can be expressed as:

$$S_{k,k-1}\left(G_{best}^{m}\right)=h\left[G_{k,best}^{m},G_{k-1,best}^{m}\right] \tag{35}$$

where $h[\cdot]$ is the constructor function of the subspace. When the particles are in the search state, those at different positions in the subspace are assigned different weights to guide them to the direction of the unexplored area of the target space where the global optimal solution is most likely to occur. The distance arrangement of different particles and global optimal particles in the subspace can be expressed as:

$$d_{\perp}\left(X_{j,k}^{m}\right)=sort\left\{\left|X_{j,k}^{m},d_{k,k-1}\left(G_{best}^{m}\right)\right|_{j=1}^{J}\right\},X_{j,k}^{m}\in S_{k,k-1}\left(G_{best}^{m}\right) \tag{36}$$

where $sort\{\cdot\}$ is the arrangement function of different particles in the subspace, $X_{j,k}^{m}$ is the m-dimensional position vector of particle j in the k-th iteration of the subspace, and J is the number of particles in the subspace.

The diversity of the particles in the search process can be improved by applying the strategy of multi-weight subspaces particles constraint. Then subspaces are searched to determine the weight of different particles based on the Euclidean distance between them. This process guides the particles to move towards the unexplored area in the target space, which increases the effectiveness of the population search and the global performance of the PSO algorithm.

3.4. The solution process of the proposed adaptive MS-PSO

The proposed adaptive MS-PSO algorithm is used for solving the multi-objective optimization model under the three scenarios previously introduced. Fig. 4 shows the flowchart of the system maintenance optimization algorithm based on the adaptive MS-PSO. The steps of this algorithm are summarized as follows:

Step 1 Initialize the particle swarm parameters, set the size of the particle swarm N, particle dimensions M and the number of iterations K, randomly initialize the position $X_{i,k}$ and speed $V_{i,k}$ of each particle, calculate the fitness value $f\left(X_{i,k}\right)$ of each particle, and determine the initial local optimal value $P_{i,0,best}$ and global optimal value $G_{0,best}$ of the particles.

Step 2 The adaptive weight optimization strategy is used to dynamically adjust the inertial weights $w(k)$ and learning factors $c_1(k)\&c_2(k)$ to provide conditions for particles to quickly converge to the global optimum $G_{k,best}^{m}$, and enable the balance between the global and local searches.

Step 3 Update the particle position $X_{i,k}^{m}$ and speed $V_{i,k}^{m}$, and calculate the fitness value of particle. The fitness values at different points form the PF. For the latter, all the possible solutions should be considered and some of them are chosen based on the decision variables of the solution set.

Step 4 The multi-weight subspace particle constraint strategy is used to set a constraint area $S_{k,k-1}\left(G_{best}^{m}\right)$ near the Euclidean distance$d_{k,k-1}\left(G_{best}^{m}\right)$ of the two generations of global optimal particles. The weight of the particles within this area changes with the vertical distance of the Euclidean distance $d_{\perp}\left(X_{j,k}^{m}\right)$, which increases the diversity of the particles during the search process.

Step 5 Recalculate the fitness value, update the local optimal value $P_{i,k,best}^{m}$ and global optimal value $G_{k,best}^{m}$ of the particles in the subspace, and select the global optimal solution from them.

Step 6 Check whether the algorithm has completed its iterations. If the number of iterations is equal to the predefined value, or the difference between the fitness value of the optimal solution from the previous iteration and that from the current iteration is smaller than a specified threshold, the current global optimal solution is output as

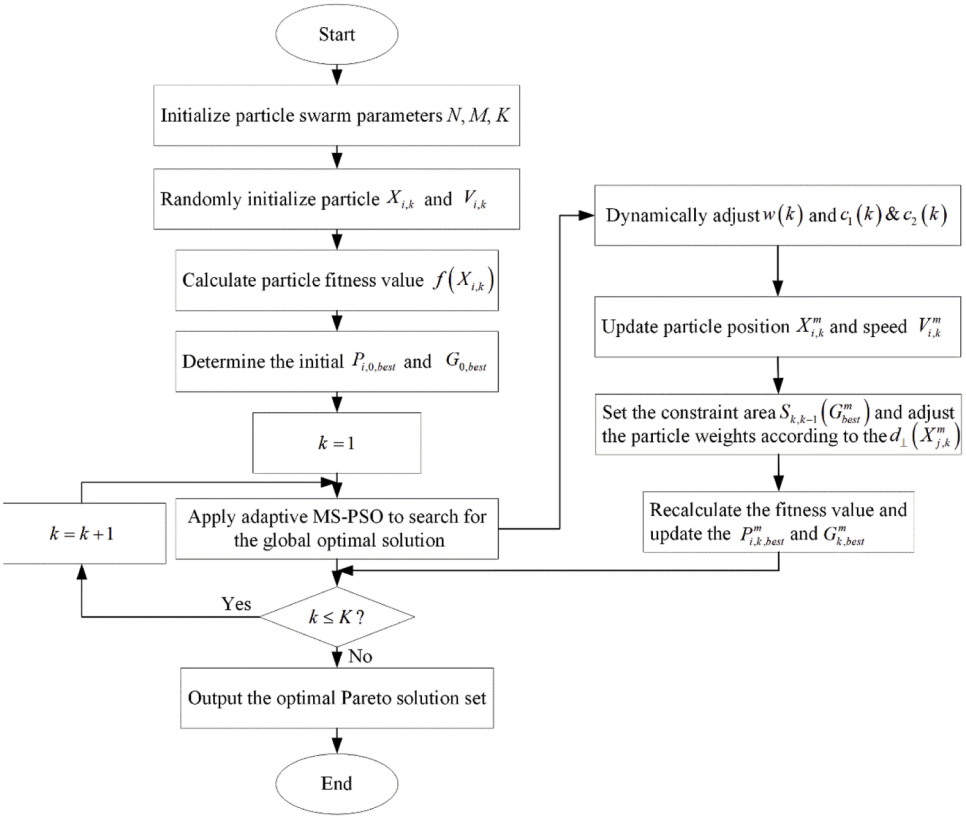

Fig. 4. Flowchart of the adaptive MS-PSO algorithm.

the final search result. Otherwise, step 2 is performed and the next round of iterations is entered.

4. Case studies

Two case studies are considered to demonstrate the effectiveness of the adaptive MS-PSO algorithm and the superiority of the proposed multi-objective maintenance strategy optimization.

4.1. Case study 1: verification of the adaptive MS-PSO algorithm

In this section, PSO, NSGA-II, and the proposed adaptive MS-PSO are compared. The ZDT1 and DTLZ1 test functions are considered for the dual-objective and three-objective problems, respectively [43].

The ZDT1 function is a widely used benchmark function for multi-objective optimization. It is a two-objective problem with a convex Pareto front, making it a standard test for evaluating the performance of multi-objective optimization algorithms. The ZDT1 function can be expressed as:

$$\begin{cases} f_1(x) = x_1 \\ f_2(x) = g(x)\cdot\left[1-\sqrt{x_1/g(x)}\right] \\ g(x) = 1+9\left(\sum_{i=2}^{n} x_i\right)\Big/(n-1) \end{cases} \tag{37}$$

where $x_1 \in [0,1]$, n is the total number of variables.

The DTLZ1 function is part of the DTLZ suite of test problems designed for multi-objective optimization. DTLZ1 is specifically challenging because it includes a high-dimensional search space and requires the optimization algorithm to converge to a Pareto front that forms a simplex. The DTLZ1 function can be expressed as:

$$\begin{cases} f_i(\mathrm{x}) = \frac{1}{2}x_1x_2\cdots x_{M-1}(1+g(x_{M:n})), i = 1,\ldots,M-1 \\ f_M(\mathrm{x}) = \frac{1}{2}(1-x_1)(1+g(x_{M:n})) \\ g(\mathrm{x}_{M:n}) = 100\left[|\mathrm{x}_{M:n}| + \sum_{j=M}^{n}\left((x_j-0.5)^2 - \cos(20\pi(x_j-0.5))\right)\right] \end{cases} \tag{38}$$

where $\mathrm{x} = (x_1, x_2, \ldots, x_n)$ is the decision variable vector, M is the number of objective functions and k is a parameter used to define the complexity of the function. The domain of each decision variable x_j is $[0,1]$.

Aiming at a fair comparison, for all the test problems, N is set to 100 and the maximum number of iterations is set to 80. For the proposed adaptive MS-PSO method, the maximum number of subspaces is set to 8. The setting parameters of the proposed method are shown in Table 1.

The inertia weight iteration curve of the MS-PSO algorithm is shown in Fig. 5. It can be observed that with the increase in the number of iterations, the inertia weight maximum value of 1.5 can be nonlinearly adjusted to the minimum value of 0.6 using the tan function. The inertia weight of the basic PSO decreases linearly with the increase in the number of iterations. When the number of iterations reaches about 60, the MS-PSO algorithm tends to be stable. Therefore, the MS-PSO algorithm has better performance in terms of efficiency than the basic PSO algorithm.

Table 1
Parameters setting of the proposed adaptive MS-PSO algorithm.

Parameter	Value
Particle swarm size	100
Maximum number of iterations	80
Variation range of inertia weight	1.5–0.6
Local learning factor change range	1.3–2.1
Global learning factor change range	1.9–1.1
Maximum number of subspaces	8

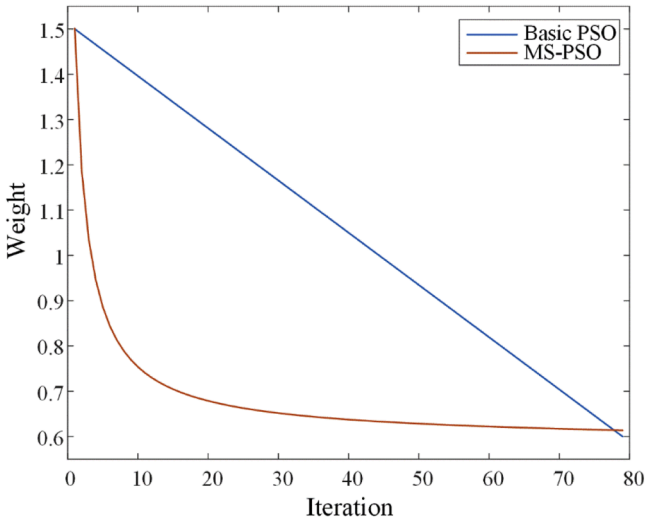

Fig. 5. Iteration curve of inertia weight.

The performances of the three considered methods are compared on dual-objective and three-objective test functions, using the parameters of Table 1. The results of the comparison are shown in Figs. 6 and 7.

Fig. 6 shows the results of the comparison between PSO, NSGA-II, and the proposed adaptive MS-PSO on the ZDT1 test function. It can be seen that the non-dominated solution set obtained by the proposed adaptive MS-PSO algorithm in the dual-objective test function is closer to the true PF and the solution set is more dispersed than the PFs of the other two algorithms. This demonstrates that the proposed method outperforms the basic PSO and NSGA-II algorithms.

Fig. 7 shows the results of the comparison between PSO, NSGA-II, and the proposed adaptive MS-PSO on the DTLZ1 test function, where the gray part denotes the true PF. It can be seen that the approximate solution set obtained by the proposed adaptive MS-PSO algorithm in the three-objective optimization problem is close to the true PF, which demonstrates that the obtained solution set is accurate and more so than those obtained by the basic PSO and NSGA-II algorithms. In addition, the obtained solutions are scattered, which shows that the proposed algorithm has satisfactory convergence and diversity.

As shown in Table 2, we randomly selected 10 solution sets from Fig. 7 to compare different optimization algorithms. The PF satisfies $\sum_{i=1}^{3} f_i = 0.5$. The closer the sum of the objective function solutions obtained by the algorithm is to 0.5, the closer the approximate solution set obtained by the algorithm is to the true PF, indicating that the solution set obtained by the algorithm is more accurate. From Table 2, we can see that the solution of the proposed adaptive MS-PSO algorithm is closer to the true PF.

Furthermore, the hypervolume (HV) and inverted generational distance (IGD) metrics are used to evaluate and compare the performances of the three algorithms.

The HV index is used to evaluate the degree to which the target space is covered by an approximation set. This is the most commonly used evaluation index. Note that a reference point is required, and the HV value is the volume of the hypercube formed between the PF and the reference point. The larger the HV value, the better the diversity and convergence of the algorithm, and the closer the solution found to the true PF. The HV indicator is calculated as:

$$HV(f^r, P) = Vol\left(\bigcup_{p\in P}[f_1(p), f_1^r] \times [f_2(p), f_2^r] \times \ldots \times [f_m(p), f_m^r]\right) \tag{39}$$

where f_i^r is the reference point and $f_i(p)$is the solution set.

The IGD index is used to evaluate the gap between the approximate

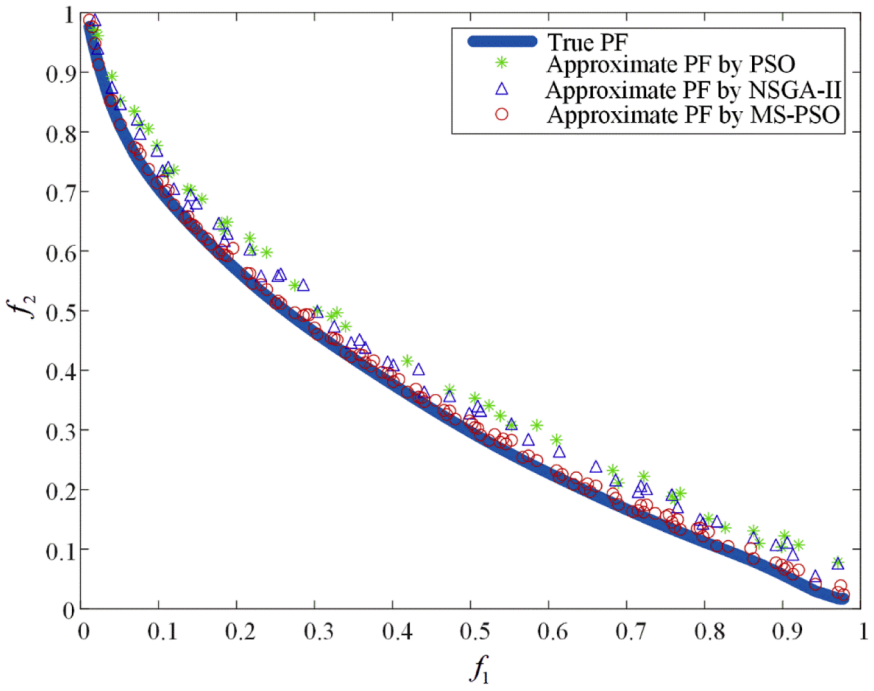

Fig. 6. Comparison between PSO, NSGA-II, and the proposed adaptive MS-PSO on the ZDT1 test function.

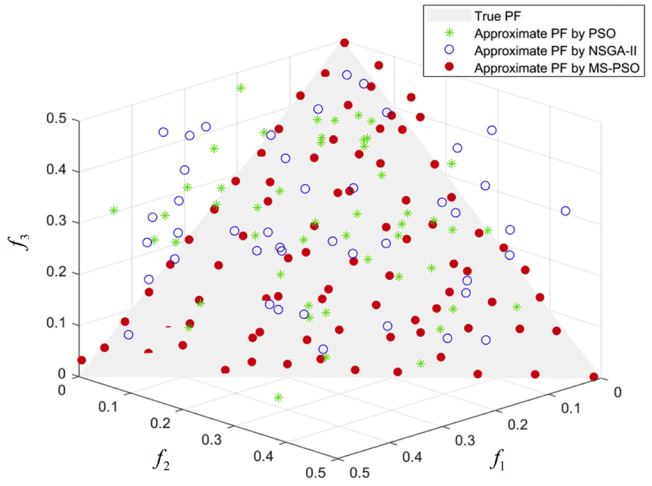

Fig. 7. Comparison between PSO, NSGA-II, and the proposed adaptive MS-PSO on the DTLZ1 test function.

Table 2
Comparison of PSO, NSGA-II and the proposed adaptive MS-PSO on the solution set of DTLZ1 test function.

$\sum_{i=1}^{3} f_i$	PSO	NSGA-II	MS-PSO
1	0.5341	0.5247	0.5060
2	0.5242	0.5232	0.5049
3	0.5293	0.5119	0.5074
4	0.5358	0.5133	0.5058
5	0.5352	0.5215	0.5132
6	0.5259	0.5287	0.5128
7	0.5331	0.5118	0.4989
8	0.5349	0.5106	0.4943
9	0.5218	0.5280	0.5007
10	0.5347	0.5190	0.5160

PF and the true PF. For each solution in the true PF, that in the approximate PF which is the closest to it is found, its Euclidean distance is calculated. The smaller the IGD value, the closer the approximate PF to the true one, the better the diversity and convergence of the algorithm. Note that the IGD calculation requires the determination of the true PF. The IGD indicator is computed as:

$$IGD(PF^*, P) = \frac{\sum_{y \in PF^*} d(y, P)}{|PF^*|} \tag{40}$$

where $d(y, P)$ is the minimum Euclidean distance between solution y and that in set P.

Tables 3 and 4 represent the results of the comparison between the PSO, NSGA-II, and the proposed adaptive MS-PSO on the ZDT1 and DTLZ1 test functions, respectively. It can be seen from Table 3 that the HV value obtained by the adaptive MS-PSO algorithm in the ZDT1 test function is larger and the IGD value is smaller compared to those obtained by the other two algorithms. This demonstrates that the approximate solution obtained by the proposed algorithm is more accurate and its approximate solution is closer to the true solution. Similar results are observed from Table 4, which shows that the proposed algorithm improves the diversity and accuracy of the solution, and it outperforms the basic PSO and classical NSGA-II algorithm in solving multi-objective optimization problems. The MS-PSO algorithm achieves a better balance between convergence and diversity by employing a multi-objective particle swarm mechanism that adjusts particle movement based on both global and local search tendencies. This leads to faster convergence toward the Pareto optimal front while maintaining a diverse set of solutions, which is critical for achieving higher HV and lower IGD values. In comparison, NSGA-II relies on a genetic algorithm

Table 3
Comparison between the performances of the PSO, NSGA-II, and the proposed adaptive MS-PSO on the ZDT1 test function.

Algorithm	HV	IGD
PSO	116.43	9.41E-02
NSGA-II	117.18	7.95E-02
MS-PSO	119.67	4.63E-02

Table 4
Comparison between the performances of the PSO, NSGA-II, and the proposed adaptive MS-PSO on the DTLZ1 test function.

Algorithm	HV	IGD
PSO	1216.79	8.47E-02
NSGA-II	1238.42	8.21E-02
MS-PSO	1241.58	5.83E-02

framework, which can sometimes struggle with maintaining diversity, and PSO can face difficulties in multi-objective optimization due to its single-swarm structure.

4.2. Case study 2: optimization of maintenance strategies for an aircraft hydraulic system

To verify the superiority of the proposed multi-objective maintenance strategy, the proposed method is applied to the A320 aircraft hydraulic system, which is one of the important onboard systems of the A320 aircraft. It is a complex system exhibiting redundancy and operating at high power. It consists of multiple sets of hydraulic systems that are independent and backing up each other. The hydraulic system failures can affect the normal operation of the system, and increase the costs and risks, such as due to flight delays and downtime. They can even threaten the flight safety. Therefore, the optimization of the maintenance strategy of the hydraulic system is needed to improve its operation reliability and availability, and to reduce its life cycle maintenance costs.

The structure diagram of the hydraulic system is shown in Fig. 8. The A320 has three independent hydraulic systems. The hydraulic system changes the low-pressure hydraulic oil in the fuel tank (FT) into high-pressure hydraulic oil through the engine driven pump (EDP) or electric motor pump (EMP). In addition, it uses the high-pressure hydraulic oil to drive the actuators of the aircraft. Some auxiliary components in the system, such as the fire shut-off valves (FSOV), accumulators (Acc), solenoid valve (SV), ram air turbine (RAT), and power transfer unit (PTU), allow the hydraulic system to safely and stably work, and help reducing the external interferences. The three hydraulic systems can independently provide 3000 PSI pressure to the pressure system.

After performing maintenance operations on the components, their condition will be improved. However, the quality of the repair is closely related to the expertise of the personnel and the condition of the repair components. In other words, the actual value of the repair quality is different from the expected repair effect, and thus this situation should be considered in the reliability modeling of repairable systems. The reliability and maintenance optimization of the components of hydraulic systems are studied using the proposed reliability model, which considers the maintenance uncertain impact. The reliability parameters of the components are shown in Tables 5 and 6. These data can be estimated from historical maintenance records.

It is assumed that the system is in a perfect state at the initial time with all components brand new. Fig. 9 illustrates the reliability trend of the hydraulic system components over time, in the absence of any maintenance operation.

It can be seen that the reliability of the components of the hydraulic system gradually decreases with its operation time. In order to ensure the required level of the system reliability and prevent possible failures, maintenance is performed for the component A (FT), component F (Acc) and component B (FSOV) at time $t = 150$ d. Considering the professional skills of the maintenance personnel and the actual condition of the components, the uncertain impact of maintenance on the component reliability are shown in Fig. 10.

It can be seen that as expected, considering the maintenance uncertain impact, the improvement of the reliability of the components is lower than without considering it. It can also be seen that simply ignoring the maintenance uncertain impact results in higher calculated reliability probabilities, leading to conservative maintenance and more likely latent failures. Lower professional skills of the maintenance technician may lead to more frequent imperfect repairs or longer repair times, thereby increasing the likelihood of system failures.

The three multi-objective optimization scenarios of Section 2.4 are analyzed with respect to the maintenance of the aircraft hydraulic systems. The maintenance costs for the different components are shown in Table 7.

To optimize the three different scenarios, the simulation parameters are set as follows: the minimum system reliability requirement is $R_0 = 0.9$, the minimum system availability requirement is $A_0 = 0.9$, and the maximum system maintenance cost rate is $MCR_{\max} = 17\$/\text{d}$. The failure threshold of different components of the hydraulic system is set to 0.6. In

Table 5
Parameters of components of the aircraft hydraulic system.

Paraments	A	B	C	D	E	F	G	H
β	3.4	4.1	6.4	3.5	7.1	2.6	4.9	5.8
γ	178	246	303	282	385	219	265	360

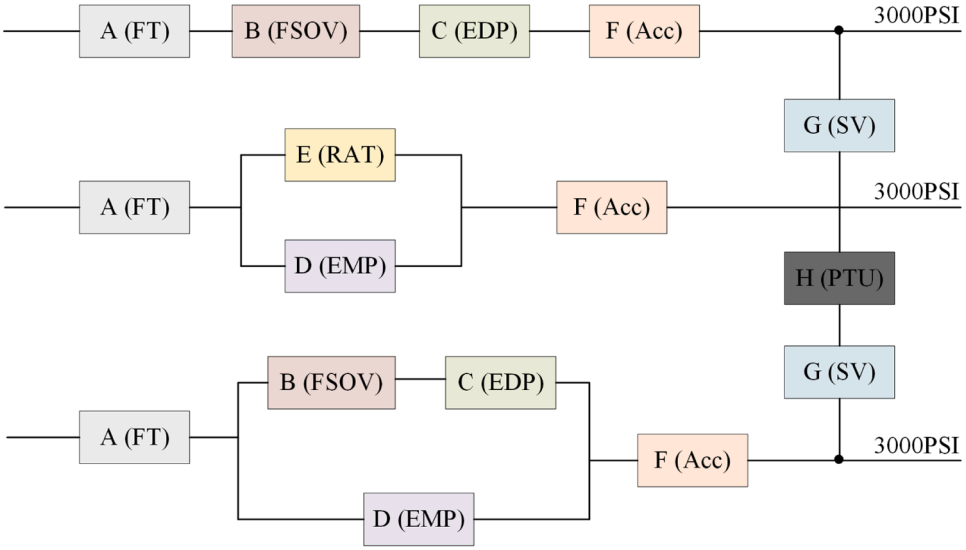

Fig. 8. Structure diagram of the hydraulic system of the A320 aircraft.

Table 6
Different maintenance actions parameters.

Maintenance actions	α	ζ	$E(\nu)$	$\sigma(\nu)$
1	14	6	0.7	0.1
2	12	3	0.8	0.1
3	2.4	0.6	0.8	0.2
4	2.975	1.275	0.7	0.2

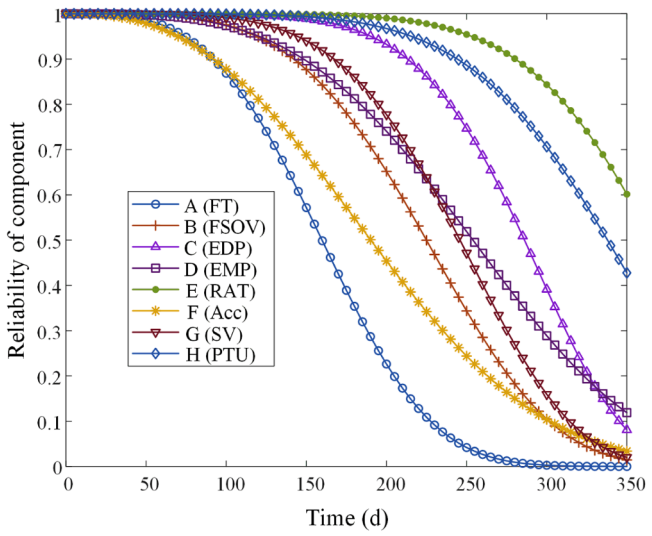

Fig. 9. Reliability of the components of a hydraulic system over time.

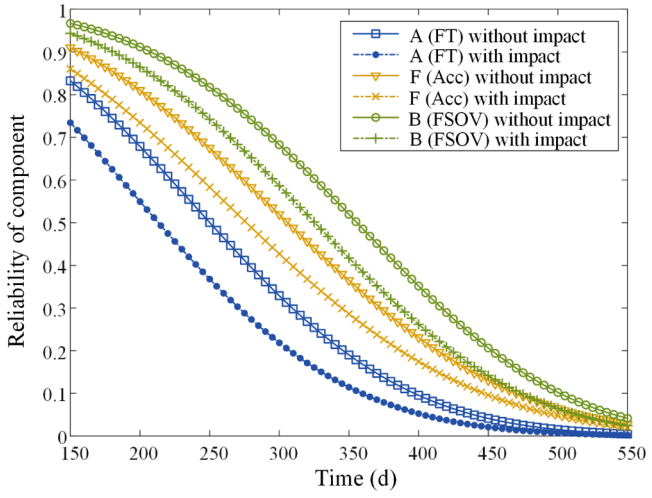

Fig. 10. Reliability of components with and without considering the maintenance uncertain impact.

Table 7
Maintenance costs of different components of the hydraulic system.

Components	$C_{im}/\times 10^2\$$	$C_{pm}/\times 10^2\$$	$C_{sp}/\times 10^2\$$	$C_d/\times 10^3\$$	$C_{om}/\times 10^3\$$
FT	57	128	12	400	100
FSOV	103	210	35		
EDP	135	278	29		
EMP	110	236	25		
RAT	94	195	19		
Acc	87	173	16		
SV	105	226	23		
PTU	76	159	18		

order to simulate the uncertainty of the failure threshold in the real world, a random variable δ is added to the component failure threshold, which follows a Gaussian distribution $N(0.6, 0.05^2)$.

The proposed MS-PSO algorithm is used to solve the multi- objectives optimization problem. For all three scenarios, a particle swarm size of 100, a maximum number of iterations of 80, a maximum number of subspaces of 10, a variation range of inertia weight of 1.5–0.6, a variation range of local learning factor of 1.2–2.3, and a variation range of global learning factor of 1.9–1.2 are used.

The first multi-objective optimization scenario consists in maximizing the availability and minimizing the MCR. The PF of the first multi-objective optimization scenario is shown in Fig. 11, and the PF optimal solution of scenario 1 is shown in Table 8.

It can be seen from Fig. 11 that the system availability and MCR obtained with various numbers of maintenance actions are different as expected. For any given number of maintenance actions, the higher the MCR, the higher the system availability, which is expected and also consistent with the actual situation. When the component number of maintenance actions is 3, the MCR is the lowest and the availability is the highest. The maintenance optimization numbers of results of scenario 1 are shown in Table 8.

It can be seen from Table 8 that in terms of MCR, when the number of maintenance actions is 4, the PF corresponding to the MCR significantly changes (from 14.89 $/d to 16.07 $/d). The lowest MCR, maintenance actions number, and system availability are 11.13 $/d, 3, and 0.9618, respectively. The maintenance times are 312, 558, and 861 d. Therefore, when the number of maintenance actions is 3, the MCR and availability are best.

Fig. 12 shows the PF for different numbers of maintenance actions in scenario 2. The optimization aims at maximizing the reliability and minimizing the MCR. It can be seen that for any given number of maintenance actions, the higher the reliability, the higher the required MCR. The combination of the MCR and reliability obtained by three maintenances is the optimal one. When the number of maintenance actions is 3, the variation range of unreliability and MCR is the smallest. Table 9 shows the maintenance optimization results of scenario 2. It can be seen that the optimal MCR, reliability, and the number of maintenance actions are 15.11 $/d, 0.9644, and 3, respectively. The maintenance times are 374, 597, and 854 d.

Fig. 13 shows the PF for different numbers of maintenance actions in scenario 3. The optimization aims at maximizing the reliability, availability and minimizing the MCR. The results are similar to those of scenarios 1 and 2. For any given number of maintenance actions, the higher the MCR, the higher the reliability and availability. A high

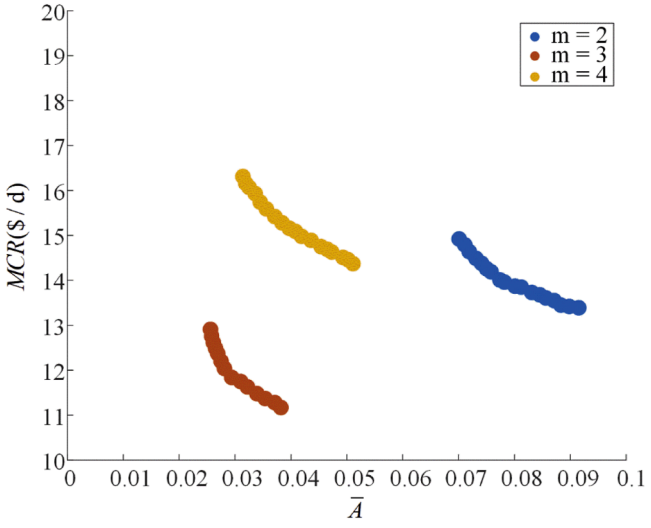

Fig. 11. PF for different numbers of maintenance actions in scenario 1.

Table 8
Maintenance optimization results of scenario 1.

Optimization objectives	Maintenance number	Maintenance Time (day)	System availability	Maintenance cost rate ($/d)
min$MCR(m,T_m)$ &max$A(m,T_m)$	2	396,784	0.9281	14.64
		384,791	0.9259	14.38
		376,813	0.9242	14.19
		387,785	0.9226	14.01
		413,796	0.9217	13.95
		401,804	0.9209	13.89
	3	283,518,896	0.9719	12.04
		276,545,874	0.9706	11.86
		280,531,882	0.9678	11.63
		293,574,839	0.9646	11.37
		312,558,861	0.9618	11.13
	4	306,463,683,875	0.9675	16.07
		338,496,702,863	0.9664	15.93
		317,485,658,839	0.9641	15.59
		343,517,702,885	0.9629	15.42
		310,475,662,847	0.9603	15.16
		352,538,715,894	0.9564	14.89

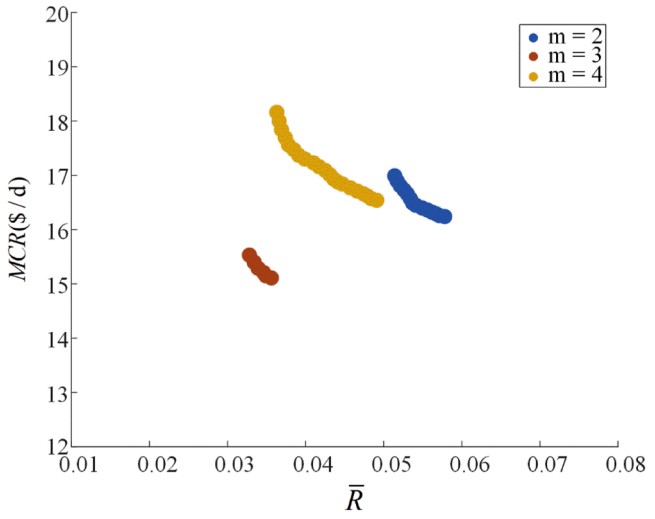

Fig. 12. PF for different numbers of maintenance actions in scenario 2.

maintenance actions indicates a high MCR. Moreover, it can be seen from Table 10 that, when the number of maintenance actions increases, the reliability and availability first increase and then decrease, while the MCR first decreases and then increases. Furthermore, the reliability, availability, and MCR reach their optimal values at a maintenance action of 3. More precisely, the MCR, reliability, and availability are 14.83 $/d, 0.9668, and 0.9632, respectively. The maintenance times are 353, 631, and 835 d

A comparison between the MCR values with and without the

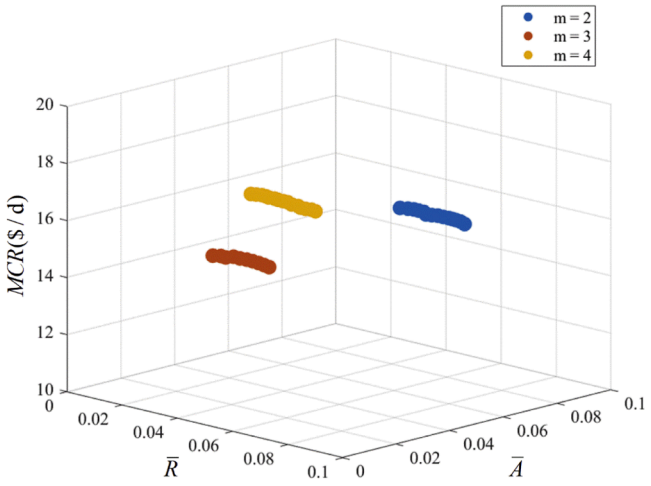

Fig. 13. PF for different numbers of maintenance actions in scenario 3.

Table 9
Maintenance optimization results of scenario 2.

Optimization objectives	Maintenance number	Maintenance Time (day)	System reliability	Maintenance cost rate ($/d)
min$MCR(m,T_m)$ &max$R(m,T_m)$	2	463,816	0.9459	16.45
		421,784	0.9451	16.41
		459,738	0.0945	16.36
		413,795	0.9438	16.32
		398,717	0.9432	16.29
		435,834	0.9429	16.26
		442,763	0.9422	16.24
	3	364,591,846	0.9672	15.53
		383,618,862	0.9664	15.40
		325,574,797	0.9661	15.29
		343,641,816	0.9654	15.21
		389,637,825	0.9651	15.15
		374,597,854	0.9644	15.11
	4	318,537,741,894	0.9543	16.77
		286,512,726,851	0.9534	16.71
		349,553,718,883	0.9526	16.65
		294,541,753,916	0.9521	16.62
		327,574,712,874	0.9516	16.57
		291,545,763,906	0.9509	16.54

Table 10
Maintenance optimization results of scenario 3.

Optimization objectives	Maintenance number	Maintenance Time (day)	System reliability	System availability	Maintenance cost rate ($/d)
min$MCR(m, T_m)$ &max$R(m, T_m)$ &max$A(m, T_m)$	2	442,839	0.9432	0.9162	15.41
		415,794	0.9425	0.9154	15.37
		423,812	0.9419	0.9149	15.34
		396,775	0.9413	0.9137	15.27
		428,783	0.9406	0.9129	15.18
	3	364,618,794	0.9689	0.9671	14.97
		337,582,816	0.9681	0.9657	14.91
		348,591,772	0.9674	0.9645	14.85
		353,631,835	0.9668	0.9632	14.83
	4	315,537,684,864	0.9586	0.9564	16.43
		284,516,641,837	0.9582	0.9559	16.37
		296,548,713,892	0.9574	0.9548	16.32
		321,545,682,849	0.9568	0.9553	16.27
		304,524,663,823	0.9561	0.9525	16.21

maintenance uncertain impact is shown in Fig. 14. It can be seen that the MCR obtained considering the maintenance uncertain impact is lower than that without considering it. This may be due to the fact that during the actual maintenance process, the quality of maintenance is related to the professional skills of maintenance personnel and the condition of the repaired components. Neglecting the maintenance uncertain impact may lead to underestimating the risk of failure of the maintained components. This increases the probability of system failure, which results in increasing the unnecessary failure maintenance expenses and system downtime costs. Considering maintenance uncertainty can more effectively formulate maintenance strategies by incorporating some unexpected situations that may occur, reduce unexpected failures and excessive downtime, and thus reduce the MCR. In addition, the increased failure probability also leads to the increase of the uncertainty loss of the system. Therefore, the MCR considering the maintenance uncertain impact is lower than the without considering it.

Fig. 15 shows a comparison between the system cumulative availability with and without considering the maintenance uncertain impact. It can be seen that the cumulative availability of the system considering the maintenance uncertain impact is higher than that without considering it. This may be due to the fact that neglecting the maintenance uncertain impact may result in underestimating the risk of failure of the maintained components, leading to the increase of the probability of system failure. By considering the maintenance uncertain impact, the proposed strategy can better adapt to real-world conditions. This allows for more realistic modeling of system behavior and the development of more robust maintenance plans, leading to higher cumulative availability. On the other hand, strategies that ignore maintenance uncertainty often rely on fixed plans, which may not adapt well to unexpected outages, leading to lower overall availability.

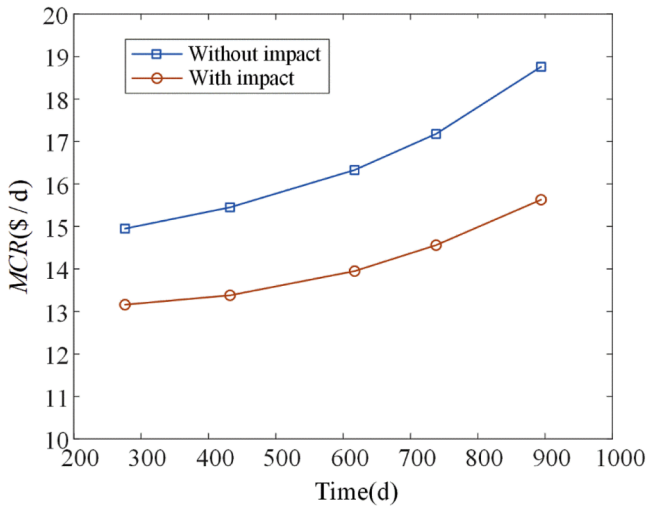

Fig. 14. Comparison between the MCR values with and without the maintenance uncertain impact.

Finally, the proposed multi-objective maintenance strategy is compared with scheduled maintenance, single objective maintenance and multi-objective maintenance strategies. The obtained results are shown in Figs. 16 and 17.

Fig. 16 shows a comparison of the system cumulative availability for different maintenance strategies. It can be seen that the system cumulative availability of the multi-objective maintenance strategy is better than that of the single-objective maintenance and scheduled maintenance strategies. This suggests that the multi-objective maintenance strategy is more effective in maintaining the operational performance of system throughout its life cycle. This may be due to the fact that the multi-objective maintenance strategy can be considered as the optimal system maintenance through its comprehensive consideration of multiple system indicators, such as system reliability, availability, and maintenance costs. In contrast, the corrective maintenance strategy only addresses issues after a failure occurs, resulting in lower availability due to increased downtime. The single-objective maintenance strategy, while optimizing one aspect, does not account for other critical factors that could affect overall system performance. Scheduled maintenance, on the other hand, relies on predetermined intervals for maintenance actions, which can lead to either excessive maintenance or the inability to prevent failures in a timely manner. Therefore, the multi-objective maintenance strategy significantly improves the cumulative availability of the system.

A comparison between the MCR results of scheduled maintenance, single objective maintenance and multi-objective maintenance strategies for different maintenance frequencies is shown in Fig. 17. It can be seen that the multi-objective maintenance has the lowest MCR, followed by the single-objective maintenance, while the corrective maintenance has the highest one. This is due to the fact that the corrective maintenance strategy, which reacts to system failures, often leads to higher costs due to unplanned repairs and longer downtimes. The scheduled maintenance involves a downtime for inspection and the replacement of components at specified intervals. This kind of maintenance plans based on empirical decisions tend to be conservative, which results in over-maintenance and poor economics. The single-objective maintenance strategy focuses on optimizing a specific factor but fails to consider other important aspects, leading to suboptimal cost management. The multi-objective maintenance strategy comprehensively considers different maintenance indicators and determines the optimal solution of maintenance time through an optimization algorithm. Thus, the optimal MCR of the system can be obtained based on ensuring its reliability and availability.

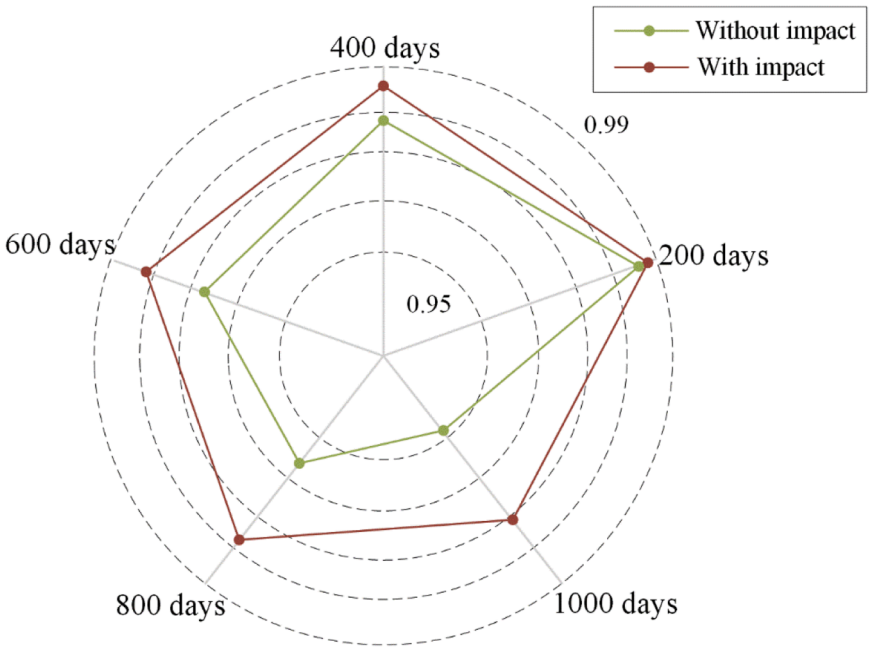

Fig. 15. Comparison between the cumulative availability with and without maintenance uncertain impact.

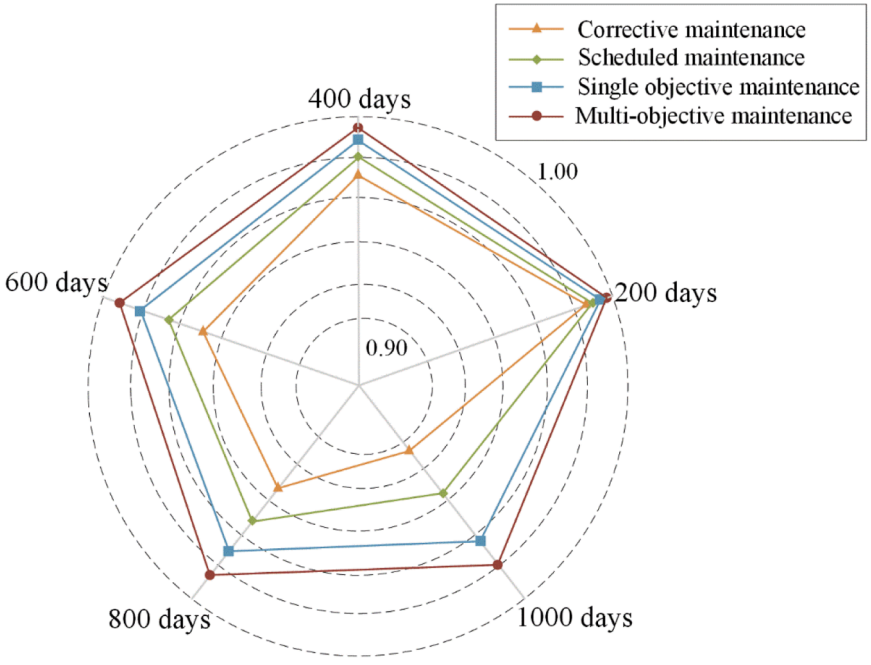

Fig. 16. Comparison of cumulative availability for corrective maintenance, scheduled maintenance, single objective maintenance and multi-objective maintenance strategies.

5. Conclusion and future research

In this study, a reliability model for multi-component repairable systems which takes the maintenance uncertain impact into consideration is proposed. It comprehensively evaluates the reliability by considering the skills of the maintenance personal and the actual condition of the components to be maintained, so as to determine the system states after maintenance and provide a basis for the formulation of the next maintenance action. Compared with reliability models that do not consider the maintenance uncertain impact, the proposed approach reduces the risk of failure of maintained components being underestimated. Then a multi-objective maintenance strategy optimization model is developed and solved using a proposed MS-PSO algorithm. The results show that the proposed MS-PSO algorithm can ensure higher uniformity and accuracy of the solution compared with NSGA-II and basic PSO. That is, the distribution of the solution on the Pareto front (PF) is uniform and closer to the true PF. Therefore, the proposed algorithm has higher performance than the NSGA-II algorithm and PSO algorithm. A case study of an aircraft hydraulic system shows that the proposed reliability modeling and maintenance strategy optimization considering the maintenance uncertain impact is effective for reducing the failure probability of the system while reducing the unnecessary

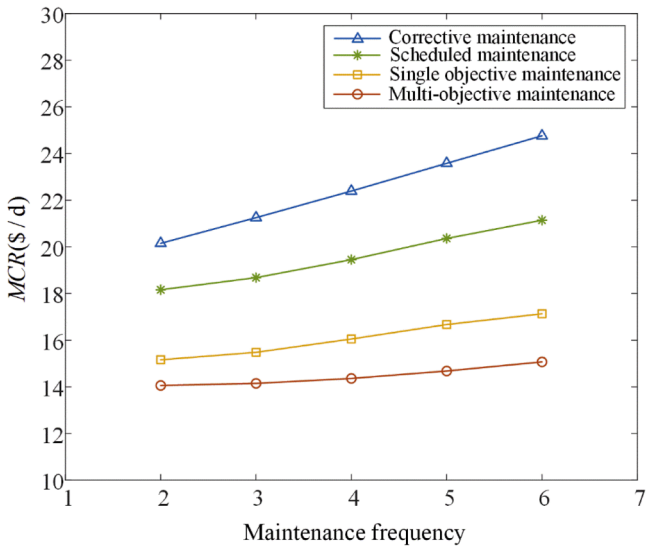

Fig. 17. Comparison of the MCR results of corrective maintenance, scheduled maintenance, single objective maintenance and multi-objective maintenance strategies.

failure repair and system downtime costs. The proposed multi-objective maintenance strategy significantly reduces the MCR and improves the system cumulative availability compared with existing scheduled maintenance and single objective maintenance strategies.

Although the proposed method provides valuable insights for the formulation of maintenance strategies considering the skills of maintenance personnel and the actual condition after maintenance, the proposed method relies on the accuracy of the input data, and the performance of the proposed method may deteriorate when the data is scarce or unreliable. In future work, the proposed method will be combined with hybrid multi-unit maintenance strategy for joint optimization.

CRediT authorship contribution statement

Yadong Zhang: Writing – original draft, Validation, Software, Methodology, Conceptualization. **Shaoping Wang:** Writing – review & editing, Supervision, Resources, Funding acquisition. **Enrico Zio:** Writing – review & editing, Supervision, Conceptualization. **Chao Zhang:** Writing – review & editing, Resources, Funding acquisition, Conceptualization. **Hongyan Dui:** Visualization, Investigation. **Rentong Chen:** Writing – review & editing, Supervision, Conceptualization.

Declaration of competing interest

The authors declare that they have no known competing financial interests or personal relationships that could have appeared to influence the work reported in this paper. All authors declare that no conflict of interest exists.

Acknowledgments

The authors would like to express their gratitude for the financial support of the National Natural Science Foundation of China (Grant No. U2233212, 52375036) and the program of China Scholarship Council (No. 202306020133).

Data availability

Data will be made available on request.

References

[1] Chen Z, Zhou D, Xia T, Pan E. Online unsupervised optimization framework for machine performance assessment based on distance metric learning. Mech Syst Signal Process 2024;206:110883. https://doi.org/10.1016/j.ymssp.2023.110883.
[2] Cai B, Wang Z, Zhu H, Liu Y, Hao K, Yang Z, et al. Artificial intelligence enhanced two-stage hybrid fault prognosis methodology of PMSM. IEEE Trans Ind Inf 2022; 18:7262–73. https://doi.org/10.1109/TII.2021.3128245.
[3] Zhang Y, Zhang C, Wang S, Dui H, Chen R. Health indicators for remaining useful life prediction of complex systems based on long short-term memory network and improved particle filter. Reliab Eng Syst Saf 2024;241:109666. https://doi.org/10.1016/j.ress.2023.109666.
[4] Kong X, Cai B, Zou Z, Wu Q, Wang C, Yang J, et al. Three-model-driven fault diagnosis method for complex hydraulic control system: subsea blowout preventer system as a case study. Expert Syst Appl 2024;247:123297. https://doi.org/10.1016/j.eswa.2024.123297.
[5] Levitin G, Xing L, Xiang Y. Optimal multiple replacement and maintenance scheduling in two-unit systems. Reliab Eng Syst Saf 2021;213:107803. https://doi.org/10.1016/j.ress.2021.107803.
[6] Zio E, Miqueles L. Digital twins in safety analysis, risk assessment and emergency management. Reliab Eng Syst Saf 2024;246:110040. https://doi.org/10.1016/j.ress.2024.110040.
[7] Cai B, Kong X, Liu Y, Lin J, Yuan X, Xu H, et al. Application of bayesian networks in reliability evaluation. IEEE Trans Ind Inf 2019;15:2146–57. https://doi.org/10.1109/TII.2018.2858281.
[8] Syamsundar A, Naikan VNA, Wu S. Estimating maintenance effectiveness of a repairable system under time-based preventive maintenance. Comput Ind Eng 2021;156:107278. https://doi.org/10.1016/j.cie.2021.107278.
[9] Zhang Y, Zhang C, Wang S, Chen R, Tomovic MM. Performance Degradation Based on Importance Change and Application in Dissimilar Redundancy Actuation System. Mathematics 2022;10:843. https://doi.org/10.3390/math10050843.
[10] Wu Q, Feng Q, Ren Y, Xia Q, Wang Z, Cai B. An intelligent preventive maintenance method based on reinforcement learning for battery energy storage systems. IEEE Trans Ind Inf 2021;17:8254–64. https://doi.org/10.1109/TII.2021.3066257.
[11] Li X, Ran Y, Chen B, Chen F, Cai Y, Zhang G. Opportunistic maintenance strategy optimization considering imperfect maintenance under hybrid unit-level maintenance strategy. Comput Ind Eng 2023;185:109624. https://doi.org/10.1016/j.cie.2023.109624.
[12] Li Y, Shi Y, Zhang Z, Lu N, Wang X, Zio E. Condition-based maintenance for performance degradation under nonperiodic unreliable inspections. IEEE Trans Artif Intell 2023;4:709–21. https://doi.org/10.1109/TAI.2022.3197680.
[13] Zhu X, Wang J, Coit DW. Joint optimization of spare part supply and opportunistic condition-based maintenance for onshore wind farms considering maintenance route. IEEE Trans Eng Manage 2024;71:1086–102. https://doi.org/10.1109/TEM.2022.3146361.
[14] Zio E. Prognostics and health management methods for reliability prediction and predictive maintenance. IEEE Trans Rel 2024;73. https://doi.org/10.1109/TR.2024.3356816. 41–41.
[15] Dui H, Zhang Y, Bai G. Analysis of variable system cost and maintenance strategy in life cycle considering different failure modes. Reliab Eng Syst Saf 2024;243: 109824. https://doi.org/10.1016/j.ress.2023.109824.
[16] Lu Y, Wang S, Zhang C, Chen R, Dui H, Mu R. Adaptive maintenance window-based opportunistic maintenance optimization considering operational reliability and cost. Reliab Eng Syst Saf 2024;250:110292. https://doi.org/10.1016/j.ress.2024.110292.
[17] Levitin G, Xing L, Dai Y. Minimizing mission cost for production system with unreliable storage. Reliab Eng Syst Saf 2022;227:108724. https://doi.org/10.1016/j.ress.2022.108724.
[18] Zhang C, Zhang Y, Dui H, Wang S, Tomovic M. Importance measure-based maintenance strategy considering maintenance costs. Eksploatacja i Niezawodność – Maintenan Reliab 2022;24:15–24. https://doi.org/10.17531/ein.2022.1.3.
[19] Li S, Yang Z, He J, Li G, Yang H, Liu T, et al. A novel maintenance strategy for manufacturing system considering working schedule and imperfect maintenance. Comput Ind Eng 2023;185:109656. https://doi.org/10.1016/j.cie.2023.109656.
[20] Ma Z, Liao H, Gao J, Nie S, Geng Y. Physics-informed machine learning for degradation modeling of an electro-hydrostatic actuator system. Reliab Eng Syst Saf 2023;229:108898. https://doi.org/10.1016/j.ress.2022.108898.
[21] Li X-Y, Li X, Feng J, Li C, Xiong X, Huang H-Z. Reliability analysis and optimization of multi-phased spaceflight with backup missions and mixed redundancy strategy. Reliab Eng Syst Saf 2023;237:109373. https://doi.org/10.1016/j.ress.2023.109373.
[22] Zuo F, Zio E, Xu Y. Bi-objective optimization of the scheduling of risk-related resources for risk response. Reliab Eng Syst Saf 2023;237:109391. https://doi.org/10.1016/j.ress.2023.109391.
[23] Cai B, Shao X, Liu Y, Kong X, Wang H, Xu H, et al. Remaining useful life estimation of structure systems under the influence of multiple causes: subsea pipelines as a case study. IEEE Trans Ind Electron 2020;67:5737–47. https://doi.org/10.1109/TIE.2019.2931491.
[24] Wang Y, Xie M, Su C. Multi-objective maintenance strategy for corroded pipelines considering the correlation of different failure modes. Reliab Eng Syst Saf 2024; 243:109894. https://doi.org/10.1016/j.ress.2023.109894.
[25] Han Y, Zhen X, Huang Y. Multi-objective optimization for preventive maintenance of offshore safety critical equipment integrating dynamic risk and maintenance cost. Ocean Eng 2022;245:110557. https://doi.org/10.1016/j.oceaneng.2022.110557.

[26] Wei Z, Zhao Z, Zhou Z, Ren J, Tang Y, Yan R. A deep reinforcement learning-driven multi-objective optimization and its applications on aero-engine maintenance strategy. J Manuf Syst 2024;74:316–28. https://doi.org/10.1016/j.jmsy.2024.04.003.
[27] Chen Z, Chen Z, Zhou D, Xia T, Pan E. Opportunistic maintenance optimization of continuous process manufacturing systems considering imperfect maintenance with epistemic uncertainty. J Manuf Syst 2023;71:406–20. https://doi.org/10.1016/j.jmsy.2023.10.001.
[28] Liu X, Cai B, Yuan X, Shao X, Liu Y, Akbar Khan J, et al. A hybrid multi-stage methodology for remaining useful life prediction of control system: subsea Christmas tree as a case study. Expert Syst Appl 2023;215:119335. https://doi.org/10.1016/j.eswa.2022.119335.
[29] Chen R, Wang S, Zhang C, Dui H, Zhang Y, Zhang Y, et al. Component uncertainty importance measure in complex multi-state system considering epistemic uncertainties. Chinese J Aeronautic 2024.
[30] Li X-Y, Huang H-Z, Li Y-F, Xiong X. A Markov regenerative process model for phased mission systems under internal degradation and external shocks. Reliab Eng Syst Saf 2021;215:107796. https://doi.org/10.1016/j.ress.2021.107796.
[31] Ruiz-Rodríguez ML, Kubler S, Robert J, Le Traon Y. Dynamic maintenance scheduling approach under uncertainty: comparison between reinforcement learning, genetic algorithm simheuristic, dispatching rules. Expert Syst Appl 2024;248:123404. https://doi.org/10.1016/j.eswa.2024.123404.
[32] Li M, Jiang X, Carroll J, Negenborn RR. A multi-objective maintenance strategy optimization framework for offshore wind farms considering uncertainty. Appl Energy 2022;321:119284. https://doi.org/10.1016/j.apenergy.2022.119284.
[33] Zio E. The Monte Carlo simulation method for system reliability and risk analysis. London: Springer London; 2013. https://doi.org/10.1007/978-1-4471-4588-2.
[34] Zhang C, Zhang Y, Dui H, Wang S, Tomovic M. Component maintenance strategies and risk analysis for random shock effects considering maintenance costs. Eksploatacja i Niezawodność – Maintenan Reliab 2023;25. https://doi.org/10.17531/ein/162011.
[35] Cai B, Zhang Y, Wang H, Liu Y, Ji R, Gao C, et al. Resilience evaluation methodology of engineering systems with dynamic-Bayesian-network-based degradation and maintenance. Reliab Eng Syst Saf 2021;209:107464. https://doi.org/10.1016/j.ress.2021.107464.
[36] Zhang Y, Cai B, Zhao Y, Gao C, Liu Y, Gao L, et al. Joint multi-objective optimization method for emergency maintenance and condition-based maintenance: subsea control system as a case study. Reliab Eng Syst Saf 2024;250:110307. https://doi.org/10.1016/j.ress.2024.110307.
[37] Lv L, Shen W. An improved NSGA-II with local search for multi-objective integrated production and inventory scheduling problem. J Manuf Syst 2023;68:99–116. https://doi.org/10.1016/j.jmsy.2023.03.002.
[38] Shehadeh A, Alshboul O, Al-Shboul KF, Tatari O. An expert system for highway construction: multi-objective optimization using enhanced particle swarm for optimal equipment management. Expert Syst Appl 2024;249:123621. https://doi.org/10.1016/j.eswa.2024.123621.
[39] Pang H, Chen K, Geng Y, Wu L, Wang F, Liu J. Accurate capacity and remaining useful life prediction of lithium-ion batteries based on improved particle swarm optimization and particle filter. Energy 2024;293:130555. https://doi.org/10.1016/j.energy.2024.130555.
[40] Cai B, Wang Y, Zhang Y, Liu Y, Ge W, Li R, et al. Condition-based maintenance method for multi-component system based on RUL prediction: subsea tree system as a case study. Comput Ind Eng 2022;173:108650. https://doi.org/10.1016/j.cie.2022.108650.
[41] Dinh D-H, Do P, Iung B, Nguyen P-T-N. Reliability modeling and opportunistic maintenance optimization for a multicomponent system with structural dependence. Reliab Eng Syst Saf 2024;241:109708. https://doi.org/10.1016/j.ress.2023.109708.
[42] Sayed A, EL-Shimy M, El-Metwally M, Elshahed M. Impact of subsystems on the overall system availability for the large scale grid-connected photovoltaic systems. Reliab Eng Syst Saf 2020;196:106742. https://doi.org/10.1016/j.ress.2019.106742.
[43] Wang Y, Gao W, Gong M, Li H, Xie J. A new two-stage based evolutionary algorithm for solving multi-objective optimization problems. Inf Sci (Ny) 2022;611:649–59. https://doi.org/10.1016/j.ins.2022.07.180.